12WCEE 2000

SEISMIC ANALYSIS OF INTEGRATED WHOLE SYSTEM WITH SOURCE, PROPAGATION PATH AND STRUCTURE

Masahiro KAWANO[1], Hiroshi DOHI[2] And Satoshi MATSUDA[3]

SUMMARY

This paper presents the forward prediction model of ground motion based on wave propagation theory and source kinematics, which can deal with more reasonable seismic damage potential assessment and seismic design of a structural system. The refined model for source-site path is expressed as the multi-layered half-space which consists of a surface layer overlying a semi-infinite random medium. The source model reflecting rupture process on the entire fault plane is expressed as the summation of the slip function occurring to subevents with the lagged times which develop in compliance with a degree of the various scale heterogeneity on the fault plane. The ground motion of an earthquake event with magnitude M=7.8 is calculated for the soil ground models at five sites and source models for six slip distribution patterns. The research into this ground motion model suggests that the source-site geometry, particularly the ratio of epicentral distance to focal depth, the impedance contrast ratio of the surface soil layer to the bedrock, the source-site distance, and the directivity effects in the source radiation are considered essential physical factors for the description of ground motion and failure pattern of structural systems.

INTRODUCTION

Strong ground motion is characterized by many physical factors associated with magnitude, the faulting process in the source region, source-site geometry, types of waves, wave propagation in heterogeneous soil and geological structures, and spatial variation of seismic waves due to local site conditions. These are considered important factors, which produce the variation of wave form, frequency content, and intensity of seismic motion. This paper intends to present a forward prediction model of ground motion based on wave propagation theory and source kinematics, which can deal with more reasonable seismic damage potential assessment and seismic design for a structural system. In the source modeling, the rupture process on the fault plane is idealized in terms of the slip function, which describes the dynamic behavior of a continuous elastic membrane (Irikura 1994, Koyama 1994, Somerville et al. 1997). The slip function on the subfault is considered as a form of asperity filter with spectral characteristics, which is very similar to Haskell-type function. The source rupture growth of an earthquake is modeled as the summation of the elementary slip functions occurring to the rupture events with the lagged times, which develop in compliance with a degree of the various-scale length of heterogeneity on the entire fault plane. This source model has the ω^{-2} spectral characteristics with spatially and temporally random fluctuations (Kawano et al. 1998 a, b).

In modeling soil sediment structure for source-site path, the direct waves and their first reflection waves are considered most reliable waves for seismic design of a structural system. Then the ground motion model will consider the problem in essential way by taking into account the two representative phenomena; the decay in amplitude in the lithosphere region and the large amplification in surface soil layer. Then the refined model of soil sediment structure for source-site path could be presented as a multi-layered half-space which consists of a surface layer overlying a semi-infinite random medium (Kawano 1993).
In this paper, from the view of the physical considerations noted above, the forward prediction model of ground motion is presented by the Green's function of the multi-layered half space overlying a semi-infinite random

[1] *Department of Architecture and Environmental Design, Kyoto University, Kyoto, Japan*
[2] *Research and Development Dept, NTT Power and Building Facilities Inc., Tokyo, JapanEmail: dohi@rd.ntt-f.co.jp*
[3] *Dept of Architecture, Faculty of Engineering, Kansai University, Osaka, JapanEmail: matsuda@ipcku.kansai-u.ac.jp*

medium and the simple source model. The ground motions of an earthquake event of magnitude M=7.8 are modeled at the five sites just above and around the fault plane for the three soil ground models and the source mode for six slip distribution patterns to elucidate the key physical laws and factors, which could describe essentially the waveform function and spectral characteristics, the site amplification, the effective mechanism radiating short period waves, and the directivity effects with the source radiation.

GROUND MOTION MODEL

Source model for rupture process on fault plane

In order to investigate how the source rupture process gives an effect on structural response, the earthquake source rupture growth is modeled. This model is presented in terms of seismic moment tensor including the starting and stopping effects of the rupture front at the *m*th fault element, using the above slip vectors and slip function with temporally and spatially random variation due to heterogeneous asperity on the fault surface as follows (Kawano et al. 1996, 1998 a, b, c);

$$M_{(m)pq}(\omega) = R_{pq} M_{0(m)} \sum_{j=1}^{N1} \sum_{k=1}^{N2} \frac{\delta_j \gamma_k}{\omega\sqrt{(\omega\Delta\tau_k)^2+1}} \frac{\sin(\omega\Delta T_j/2)}{\omega\Delta T_j/2} \times \exp\left[-i\left\{\omega\tilde{t}_j + \omega\tau_k + \tan^{-1}(\omega\Delta\tau_k) + \pi/2\right\}\right] \tag{1}$$

$$\tilde{t}_j = \sum_{l=1}^{j-1}\Delta T_l + \Delta T_j/2, \quad \tau_k = \sum_{l=1}^{k-1}\Delta\tau_l, \quad M_{0(m)} = \mu\,\Delta u'_{(m)} L_{(e)} W_{(e)}$$

where $M_0(m)$, $\Delta u'_{(m)}$, R_{pq} and μ are seismic moment, average slip displacement, radiation pattern and shear rigidity at the *m*th fault element, and ΔT_j and $\Delta\tau_k$ are the fluctuating rupture time and rise time due to the small-scale heterogeneity on the fault plane, ω is the frequency, N_1 and N_2 denote the event number and the fluctuating number associated with building up dislocation at the *m*th fault element. δ_j and γ_k are the weighting factors for the dislocation amplitude. $\{\delta_j\}$, $\{\gamma_k\}$, $\{\Delta T_j\}$ and $\{\Delta\tau_k\}$ in Equation (1) are considered random variables with a uniform distribution, the coefficients of variation of which are taken to be 0.2. N_1 and N_2 in Equation (1) are set to be 5 so that the source model includes the maximum frequency component of up to 10 Hz by producing a short fluctuating rise time $\Delta\tau_k$.

For the reference case of this study, the source rupture process of an earthquake of Magnitude M=7.8 is modeled for a rectangular fault plane with length L=100 km and width W=50 km placed in a semi-infinite homogeneous region as shown in Figure 1. The fault plane is fixed with strike direction angle 0^o and dip direction angle 45^o. The rake angle is 0^o. The hypocenter is located at the lower left corner of the fault plane at a depth of 37.6km. The seismic moment of the earthquake is $M_0 = 5.0 \times 10^{27}$ dyne•cm. The fault plane is divided into N_w x N_L =15x25 subfaults with equal area $\Sigma_{(m)} = \Sigma_e = L_e$ x W_e as shown in Figure 2. The total seismic moment is distributed on each subfault in proportional to the random numbers δ_j. The average slip over the entire fault plane is 222 cm. In this study, the source rupture propagation and growth pattern is supposed as shown in Figure 2. The large fault plane is divided by five fault segments of an equal area with several fault elements. The source rupture initiates at the left corner of the first segment, propagates radially with a random velocity with average 3km/s and arrives at the neighboring segments. The source rupture propagation of radial mode is repeated on each fault segment. The seismic moment is assumed to be released at the every time when the source rupture front arrives at the center point on the fault element.

The source rupture growth on the entire fault plane may be modeled as the sum of elementary seismic moments occurring with the random lagged times $t_r(\xi_{(m)})$ to the rupture-events on the fault surface. Then the source spectra of the large-event is shown to be

$$S_0(\omega) = \left| \sum_{j=1}^{N} \dot{M}_{0(m)}(\omega)\, \exp\left[-\omega\, t_r(\xi_{(m)})\right] \right| \tag{2}$$

The time histories and spectrum of large earthquake of Equation (2) are shown in Figure 3. It is shown that the spectra of the large earthquake are flat at the lower frequencies and are proportional to the square root of the spectra at the higher frequencies.

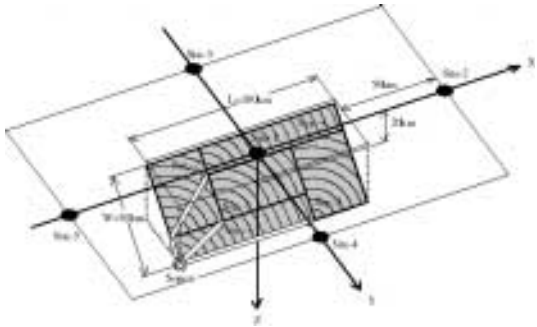

Figure 1 Geometric relation between causative fault and observation sites

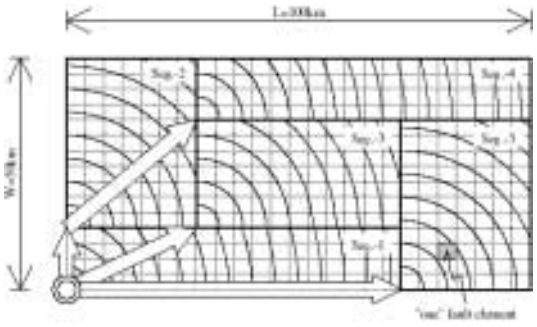

Figure 2 Rupture propagation and growth pattern on fault plane

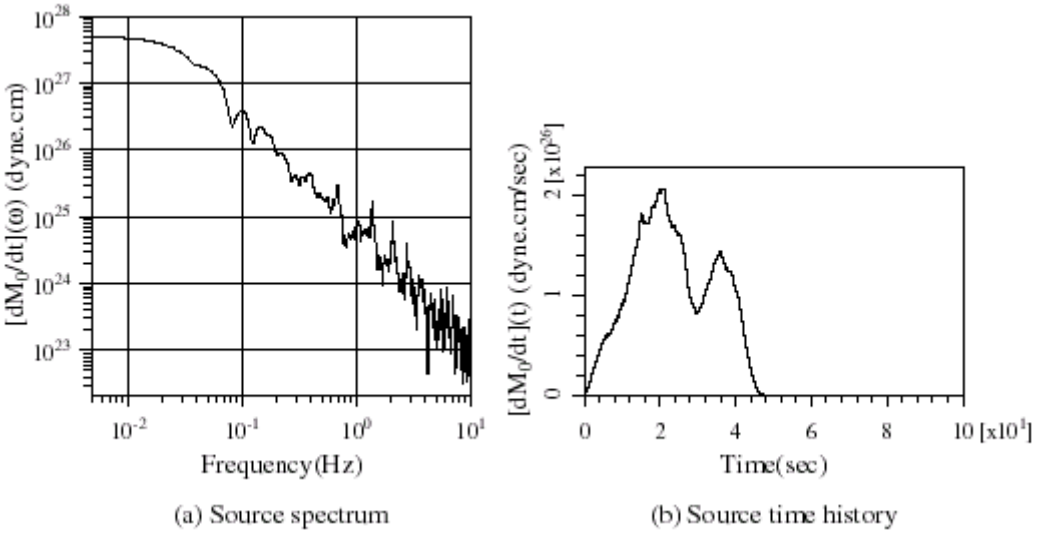

Figure 3 Source spectrum and time history of total seismic moment released over entire fault plane

Soil sediment structure model for source-site path

Since the three-dimensional geometrical structure from source to site is generally complicated, the significant findings are required to obtain the general physical laws governing the seismic wave propagation. Thus the one of major problems in the theoretical modeling of ground motion is how to present a refined soil sediment structure model for source-site path.

In this study, the direct waves and their first reflection waves are considered most reliable waves for seismic design of a structural system, and the ground motion model will consider the problem in essential way by taking into account the two representative phenomena; the decay in amplitude in the lithosphere region and the large amplification in surface soil layer. Then the refined model of soil sediment structure for source-site path could be presented as a multi-layered half-space which consists of a surface layer overlying a semi-infinite random medium.

Ground motion model

The ground motion is calculated for the rupture events occurring on the 375 subfaults of a rectangular fault plane in a semi-infinite homogeneous medium as shown in Figure 1. When $\Delta u_{(m)}(\boldsymbol{\xi},t)$ takes place at the center point $\boldsymbol{\xi}_{(m)}$ located on a subfault $\Sigma_{(m)}$, the *n*th component of displacement $u_{(m)n}(\mathbf{x};t)$ at observation point x and time t may be represented by the convolution integral as

$$u_{(m)n}(\mathbf{x},t) = M_{(m)pq}(t)\frac{\partial}{\partial \xi_q} G_{np}(\mathbf{x},t;\boldsymbol{\xi}_{(m)},0) \tag{3}$$

where $G_{np}(\mathbf{x}, t ; \boldsymbol{\xi}_{(m)}, 0)$ presents the Green's function of the *n*th component of displacement at the position at point and time t when the unit impulse is applied in the *p* direction at the center point $\boldsymbol{\xi}_{(m)}$ located on the *m*th fault element and time t=0. $M_{(m)pq}(t)$ is described by the source rupture process model presented in Section 2.1. Then the ground motion may be expressed by the summation of seismic waves radiated from all the rupture events on the entire fault plane as

$$u_n(\mathbf{x},t) = \sum_{m=1}^{N} u_{(m)n}(\mathbf{x};\ t - t_r(\xi_{(m)})) \tag{4}$$

in which $\boldsymbol{\xi}_{(m)}$ and $t_r(\boldsymbol{\xi}_{(m)})$ are the center point and dislocation starting time on the *m*th fault element $\Sigma_{(m)}$. In this ground motion modeling, the source directivity effects could be realized by the two time differences with wave propagation; the one is the arriving time difference at the site on the two wave motions radiated from the starting and stopping phases; the other is the traveling time difference at the site on wave motions radiated from the different subfault on the fault plane. Then such directivity effects could be produced with the surface integration of wave motions over the entire fault plane, which are expressed by the convolution of Green's function and source model reflecting the irregular rupture process on the entire fault plane.

NUMERICAL EXAMPLE

The ground motions calculated by Equations (3) and (4) are shown for the three soil sediment structure models at the five observation sites under the fault-site geometry relation in Figure 1. The site 1 is situated just above the fault plane, and the sites 2, 3, 4, and 5 are located around on the fault-site geometry. The stiff (G1), medium (G2) and soft (G3) soil sediment structure models as shown in Table 1 are supposed at each site. The amplification factors of them are shown in Figure 4.

Table 1-1 Stiff soil sediment structure model (G1)

Depth H(m)	P-wave velocity Vp(m/s)	S-wave velocity Vs(m/s)	Density ρ(g/cm3)	Damping factor h(%) Vp	Damping factor h(%) Vs
0-10.0	2.575	1.000	2.00	1.000	1.000
10.0-2010.0	2.800	1.500	2.30	0.500	0.500
2010.0-	5.700	3.000	2.60	0.250	0.250

Table 1-2 Medium soil sediment structure model (G2)

Depth H(m)	P-wave velocity Vp(m/s)	S-wave velocity Vs(m/s)	Density ρ(g/cm3)	Damping factor h(%) Vp	Damping factor h(%) Vs
0-3.0	0.630	0.200	1.80	1.000	1.000
3.0-10.0	1.000	0.300	2.00	1.000	1.000
10.0-14.0	1.460	0.450	2.00	1.000	1.000
14.0-27.0	2.130	0.450	2.10	1.000	1.000
27.0-33.0	2.130	0.690	2.20	1.000	1.000
33.0-45.0	2.130	0.450	2.10	1.000	1.000
45.0-70.0	2.750	0.640	2.50	0.167	0.500
70.0-139.0	2.750	0.780	2.60	0.167	0.500
139.0-150.0	2.350	0.610	2.60	0.167	0.500
150-500	2.575	1.055	2.40	0.155	0.417
500-800	2.800	1.500	2.20	0.143	0.333
800-900	4.250	2.850	2.30	0.125	0.333
900-5000	5.700	3.200	2.45	0.100	0.200
5000-18000	6.000	3.460	2.80	0.038	0.083
18000-	6.700	3.870	3.00	0.029	0.063

Table 1-3 Soft soil sediment structure model (G3)

Depth H(m)	P-wave velocity Vp(m/s)	S-wave velocity Vs(m/s)	Density ρ(g/cm3)	Damping factor h(%) Vp	Damping factor h(%) Vs
0-40.0	0.630	0.150	1.60	2.500	2.500
40.0-70.0	1.000	0.250	1.70	2.500	2.500
70.0-90.0	2.130	0.450	1.90	5.000	5.000
90.0-100.0	2.575	1.000	2.00	1.000	1.000
100.0-2100.0	2.800	1.500	2.30	0.500	0.500
2100.0-	5.700	3.000	2.60	0.250	0.250

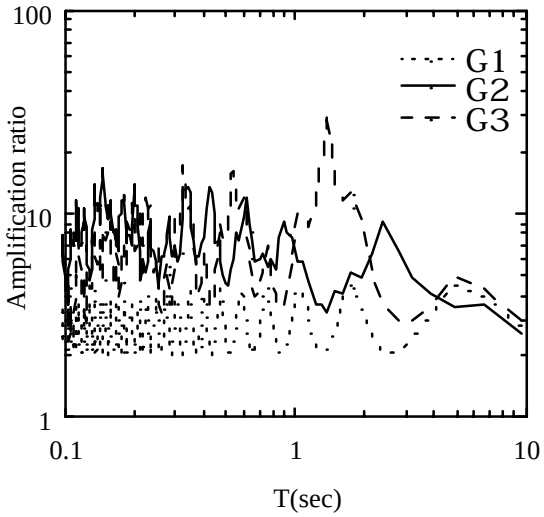

Figure 4 Site amplification ratio for three soil sediment structure models (G1:stiff, G2:medium, G3:soft)

RESULTS AND DISCUSSION

Source rupture pattern and wave form function

Figure 5 shows the variations in acceleration time histories of ground motions for NS component at all the observation sites. From these figures, it should be noted that there are significant differences in the waveforms, amplitude levels, and duration times among the ground motions at nearby sites and distant sites. The main differences are caused by the source-site geometry, the source-distance, the site effect, and the directivity in the source radiation. In the case where the site 1 is located just above the rupture fault, the dynamic faulting process reflects directly on the time histories of ground motion. The directivity effects with source radiation are responsible for the remarkable difference among the maxima of ground motions at all the observation sites. The Doppler effects with source rupture propagation produce a large difference in the time histories of ground motions and structural responses. They are increased in the forward direction of the rupture propagation compared to the backward; they increase in up-Doppler effect for the sites 2 and 5, and decrease in down-Doppler effect for the sites 3 and 4. The arrival times and shapes of seismic wave motions vary with the rupture propagation distance and the radiation pattern which is described by the relative angles between the observation site and fault element.

In the case where the sites 2, 3, 4, and 5 are at 50 km away from the side edge of the fault in the horizontal projection, the ground motions show weak transient time histories with lower amplitudes and longer durations than those at the site 1. This is because they are situated at a relatively long distance from the fault region to reduce the transient source radiation effect.

The above results confirm that the basic waveform function depends on the source-site geometry, and that the amplitude level and the duration time of ground motion are described by the magnitude, the characteristics of the soil sediment structure, the source-site distance, and the source property. In particular, the ratio R/H, the source-site distance, the impedance contrast ratio α_m, the source directivity, and the source asperity describe directly the transient state, wave pattern appearance of body waves and surface waves, peak amplitude, and duration time of ground motion. They are found to be the key physical factors, which would describe the essential characteristics of ground motion for seismic safety assessment and seismic design of a structural system.

Source rupture pattern and structural response

Figure 6 shows the velocity response spectra of ground motions for NS component to the slip distributions on five fault segments, and to the summed slip distribution over the entire fault plane at all the observation sites. Those spectra show that the transient faulting process has a tremendous effect on the structural responses especially at the site 1. They have large maxima about 200 kine in the short period range from 1.5 to 2.0 sec. The slip distribution on the segment 3 affects greatly the response spectra level. The response spectra at the sites 2 and 5 are mainly governed by the slip distributions on the fault segment 4 and the fault segments 2, 4, respectively. The peak response spectra of the sites 1, 2, and 5 do not always appear at the dominant periods of soil sediment structure model, and the response spectra levels between radial and tangential components are very different. These results suggest that the dynamic characteristics with source rupture, the source-site geometry and the source-distance are very important factors to strongly related to the failure patterns of structures to seismic ground motions.

If the structural systems in the nearby field are subjected to pulse-like seismic waves with high amplitude and very short duration radiated from the strong asperities, they could quickly fail by a few times of inelastic excursion to the high yield response level.

In contrast to the above, the ground motions at the sites 3 and 4 are less affected by the transient source movement. The peak responses of ground motions at those sites appear at the almost dominant period range from 2.0 to 3.0 of soil sediment structure model. Under this source-site geometry, surface waves are responsible for the resulting long tails in the waveform functions, which are produced by multiple reflection and refraction during wave propagation in the long source-site distance. If the structural systems are subjected to those types of seismic waves with longer duration and even lower amplitude than the site 1, they could fail by through cumulative damage caused by many cycles of hysteretic oscillation in the elasto-plastic range.

CONCLUSIONS

The forward prediction model of ground motion based on wave propagation theory and kinematic source model has been developed for seismic analysis of an integrated whole system with source, soil ground and structure. In the theoretical modeling of ground motion, the refined model of soil sediment structure from source to site is expressed as a multi-layered half-space which consists of a surface layer overlying a semi-infinite random medium. The source rupture process model is expressed as the summation of the slip functions occurring with the lagged times to subevents which develop in compliance with a degree of random small-scale heterogeneity on the fault plane.

In order to show how the variation of characteristics of ground motions affects structural response, the ground motions of an earthquake event of magnitude M=7.8 are calculated for the three soil ground models and the six slip distribution patterns. The research into the ground motion model suggests that the magnitude, the source-site geometry, especially the ratio of epicentral distance to focal depth, the impedance contrast ratio of the surface soil layer to the bedrock, the source-site distance, and the directivity effects of the source radiation are considered as the key physical factors which would play an essential role for the description of ground motion and failure pattern of a structural system.

The ground motion model presented here could predict reasonably the seismic damage potential of all kinds of structures and facilities, integrating source, wave propagation path and site. In particular, the upper and lower bounds of spectral responses through sensitivity analysis for the key physical factors describing ground motion would contribute to a more reasonable seismic safety estimation and seismic design of a structural system. In this study, the influence of topographic irregularities in the surface soil layer is not considered in the theoretical modeling of ground motion. The prediction potential of the ground motion model will be increased if such local site effects are reasonably included in the refined model of propagation path from source to site.

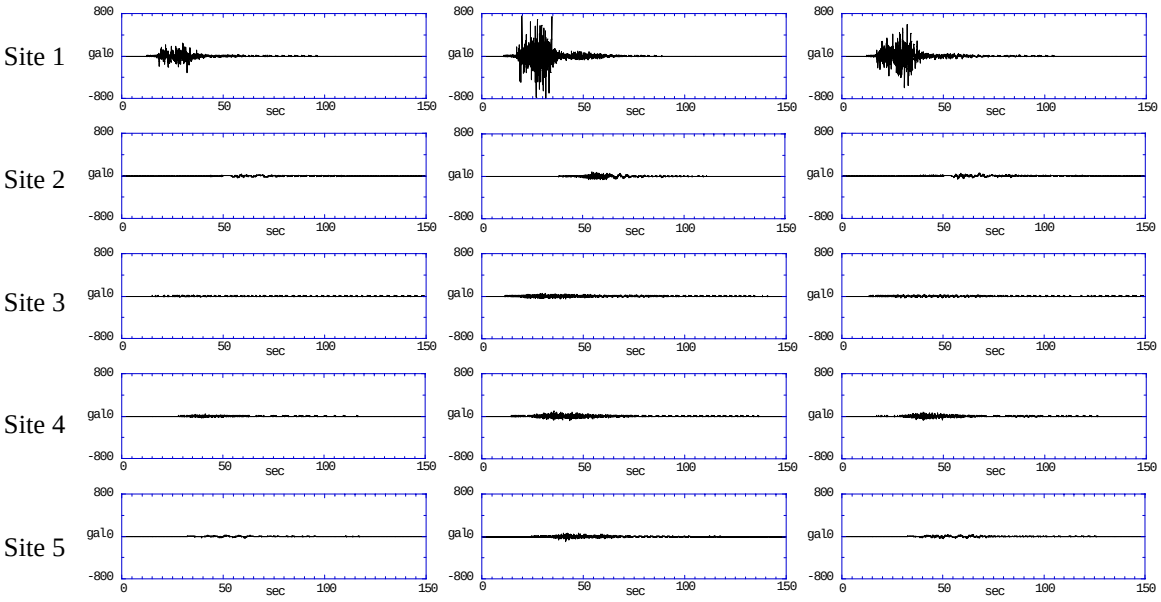

Soil site model G1 **Soil site model G2** **Soil site model G3**

Figure 5 Acceleration time histories of ground motions of NS component at all the sites

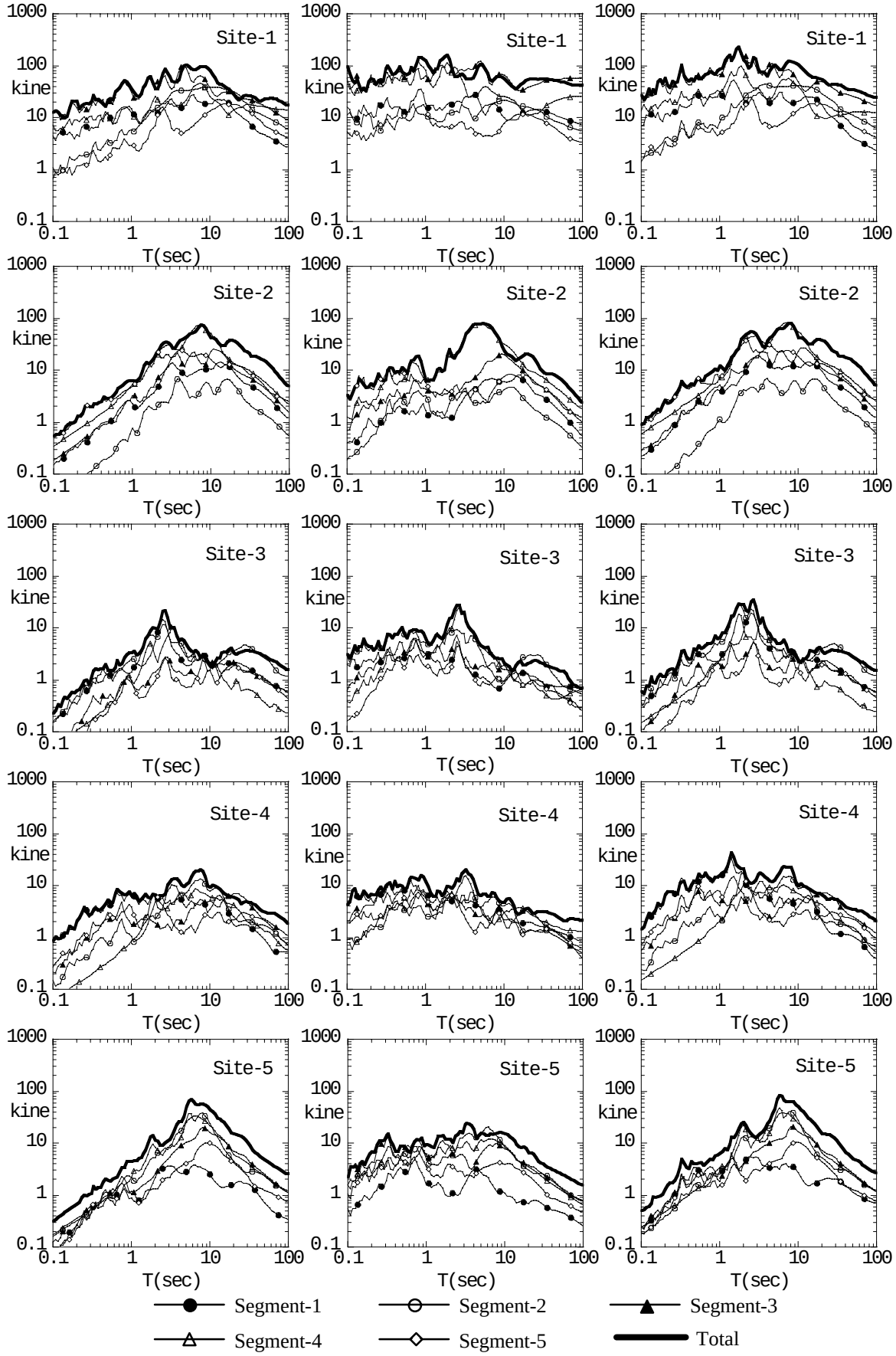

Figure 6 Velocity response spectra of ground motions of NS component for slip distributions on each fault segment and entire fault plane

REFERENCES

Irikura K. (1994) “Earthquake source modeling for strong motion prediction” *Zishin, Journal of the Seismological of Japan*, Vol. 46, No.4, pp495-512.

Kawano M. (1993) “Seismic wave propagation in a homogeneous random medium” *Earthquake motion and ground conditions*, Architectural Institute of Japan (AIJ*)*, pp79-95.

Kawano M, Dohi H, Matsuda S.(1996) “A study on ground motion for seismic design based on wave propagation theory and source dynamics” *Proceedings of 11WCEE*, No. 716.

Kawano M, Dohi H, Matsuda S. (1998a) “Study on ground motion above source region during the 1995 Hyuogo-ken Nanbu earthquake” *Proceedings of 11ECEE*, 94.

Kawano M, Dohi H, Matsuda S. (1998b) “Simultaneous simulation test against observed ground motions of the 1995 Hyogo-ken Nanbu Earthquake on the basis of wave propagation in multi-layered half space” *ESG 1998 Special volume on simultaneous simulation for Kobe* , SS-17, pp135-142.

Kawano M, Asano K, Dohi H, Matsuda S.(1998c) “Structural response based on ground motion model with consideration of heterogeneous slip distribution on fault plane” *Proceedings of 10JEES (Japanese)*, pp713-718.

Koyama J. (1994) “General discription of the complex faulting process and some empirical relations in seismology” *Journal of Physics of the Earth*, Vol. 42, pp103-148.

Somerville P. G., Smith N. F., Graves R. W., and Abrahamson N. A. (1997) “Modification of empirical strong ground motion attenuation relations to include the amplitude and duration effects of rupture directivity” Seismological Research Letters, Vol. 68, pp199-222.